Exploration of Unknown Scalar Fields with Multifidelity Gaussian Processes Under Localization Uncertainty

Demetris Coleman, Shaunak D. Bopardikar, Vaibhav Srivastava, and Xiaobo Tan

Abstract-Autonomous marine vehicles are deployed in oceans and lakes to collect spatio-temporal data. GPS is often used for localization, but is inaccessible underwater. Poor localization underwater makes it difficult to pinpoint where data are collected, to accurately map, or to autonomously explore the ocean and other aquatic environments. This paper proposes the use of multifidelity Gaussian process regression to incorporate data associated with uncertain locations. With the proposed approach, an adaptive sampling algorithm is developed for exploration and mapping of unknown scalar fields. The reconstruction performance based on the multifidelity model is compared to that based on a single-fidelity Gaussian process model that only uses data with known locations, and to that based on a single-fidelity Gaussian process model that ignores the localization error. Numerical results show that the proposed multifidelity approach outperforms both singlefidelity approaches in terms of the reconstruction accuracy.

I. INTRODUCTION

With increasingly complex mobile robotic systems, autonomous exploration has grown into a linchpin problem with varying complexity. It has applications including localization and mapping [1], search and rescue [2], multi-target search [3], and adaptive sampling [4]. When exploring a spatial field, Gaussian process (GP) regression is a common tool used to efficiently reconstruct the field as a function of the position without measuring every point. It enables the development of sampling strategies that help decide the most informative points to sample based on previously observed data. These strategies can be beneficial in many marine applications where vehicles are deployed to collect spatiotemporal data such as temperature, fish population density, or algae concentration.

When a vehicle performs underwater sensing, poor localization (GPS signal is degraded underwater) makes it difficult to pinpoint where the data are collected. The localization uncertainty also makes it challenging to accurately map and autonomously explore the underwater environments. In many cases, the position of the vehicle has to be estimated with dead reckoning. Standard Gaussian process regression assumes precise inputs (position and time for a spatio-temporal process), which is no longer directly applicable. Prediction with localization uncertainty can be obtained as a posterior predictive distribution using Bayes' rule, but it

The work was supported in part by National Science Foundation (ECCS 2030556).

Demetris Coleman, Vaibhav Srivastava, Shaunak D. Bopardikar, and Xiaobo Tan are with the Department of Electrical and Computer Engineering, Michigan State University, East Lansing, MI 48824, USA. Email: colem404@msu.edu (D.C.),shaunak@egr.msu.edu (S.D.B.),vaibhav@egr.msu.edu (V.S.), xbtan@egr.msu.edu (X.T)

generally has no analytical closed-form solution and must be approximated [5], [6].

Several researchers have proposed different methods for handling uncertainty in the inputs of a GP. In [5], Monte Carlo sampling and Laplace's method were proposed to approximate the posterior predictive statistics of GP regression for sensor networks with observations under localization uncertainty. The authors of [6] proposed an algorithm that combines Jacobi over-relaxation and discrete-time average consensus for use for distributed sensor networks under localization uncertainty. In [7], GP regression models where inputs are subject to measurement errors were investigated and a kernel that accounts for localization error was introduced. The authors of [8], [9] considered GP training with noisy input that is corrupted by i.i.d. Gaussian noise. In [10], the authors proposed an upper-confidence bound Bayesian optimization algorithm that uses a GP with probability distributions as inputs to deal with problems where the measurement and test locations are uncertain. An approach that uses the expectation of covariance matrices and keeps an analytical posterior distribution over functions is investigated to make predictions for uncertain inputs with Gaussian processes and learn from uncertain training sets in [11]. The previous works largely consider a constant noise distribution and do not focus on tasks where a mobile sensor is used to reconstruct a measurement field.

In this work, we aim to design an exploration algorithm for scalar measurement fields that accounts for and achieves accurate reconstruction under localization uncertainty. The problem is motivated by applications such as finding hotspots or mapping harmful algae blooms with underwater vehicles such as underwater gliders [12]-[14] and gliding robotic fish [15], [16]. These robots have energy-efficient motion that allows them to operate for long periods of time, but requires that they spend significant time underwater, which often causes them to experience large localization errors from the loss of access to the GPS signal. In many cases, standard adaptive sampling algorithms based on GP regression produce sample locations for a vehicle to visit and collect data. Due to the necessity of vehicles to travel between sampling locations, intermediate data can be collected along the way. Most works disregard this data. Even when such data have associated locational uncertainties, the data may still provide valuable information and collecting it could save resources such as time and energy, especially for slow moving vehicles such as underwater gliders and gliding robotic fish.

The key contribution of this work is a simple, yet effective approach for incorporating intermediate data associated with

possibly uncertain locations into a GP. To do this, we propose an approach that leverages multifidelity GP regression to model the environment through multiple correlated GPs associated with different levels of localization uncertainty. The key novelty in our approach lies in the use of the multifidelity GP framework based on the accuracy of the localization.

The idea of multifidelity GPs stem from the works of [17], [18] and have gained attention in recent years as a modeling tool [3], [19]–[22]. The original motivation for the multi-fidelity GPs is to approximate the high-fidelity data in computationally efficient manner by using surrogate models whose accuracy drops as they become computationally cheaper. Recent works have shown that the multifidelity GP model extends nicely to sensing with downward facing cameras where fidelity is dependent on the vertical distance from a 2D field being surveyed by a vehicle [3], [22].

A notable difference between the present work and the multifidelity models presented in [17], [18] is the source of the difference in fidelity levels. In the aforementioned works [3], [17], [18], [22], the fidelity level is caused by the output data from less accurate models or lower quality sensing given the true input data, whereas the fidelity in the present work is due to inaccurate input data. The present work seeks to leverage this lower fidelity input data to aid in efficiently reconstructing a spatial measurement field. Leveraging the proposed approach and the ergodic metric [23], we design an adaptive sampling algorithm and show that the proposed approach is able to lower the reconstruction error when measured by the root-mean-squared error.

The remainder of this paper is structured as follows. Section II gives a brief review of GP regression. Section III describes the problem and presents the proposed multifidelity model, followed by a description of an adaptive sampling algorithm in IV. A simulation study is conducted in the Section V and concluding remarks are given in Section VI.

II. REVIEW OF GAUSSIAN PROCESS REGRESSION

GP regression is a tool for function approximation that is commonly used to reconstruct spatial fields. It is popular due to its basis in Bayesian statistics and ability to not only predict the value of a function at an unmeasured sample point, but also provide a confidence level associated with the prediction.

A GP is fully specified by a mean function $m(\mathbf{x}): \mathbb{R}^d \to \mathbb{R}$, and a covariance function $K(\mathbf{x}, \mathbf{x}', \theta): \mathbb{R}^d \times \mathbb{R}^d \times \mathbb{R}^p \to \mathbb{R}_{\geq 0}$ (the dependence on θ will be suppressed for brevity), with hyperparameters $\theta \in \mathbb{R}^p$, for any input vectors $\mathbf{x}, \mathbf{x}' \in \mathbb{R}^d$. Given a set of input vectors $\mathbf{X} = [\mathbf{x}^{[1]}, \dots, \mathbf{x}^{[n]}]$ and, an associated set of scalar measurements $\mathbf{y} = [\tilde{\nu}^{[1]}, \dots, \tilde{\nu}^{[n]}]^T$ assumed to have an additive, zero-mean Gaussian noise, the posterior mean and variance of a Gaussian process can be predicted at any set of test vectors $\mathbf{X}^* = [\mathbf{x}^{*[1]}, \dots, \mathbf{x}^{*[q]}]$. The mean $\mu(\mathbf{X}^*)$ and variance $\Sigma(\mathbf{X}^*)$ at inputs \mathbf{X}^* can be predicted via the equations (see [24] for more details)

$$\mu(\mathbf{X}^*) = m(\mathbf{X}^*) + K(\mathbf{X}^*, \mathbf{X})[K(\mathbf{X}, \mathbf{X}) + \sigma_n^2 I]^{-1}(\mathbf{y} - m(\mathbf{X}))$$
(1)

$$\Sigma(\mathbf{X}^*) = K(\mathbf{X}^*, \mathbf{X}^*)$$

$$- K(\mathbf{X}^*, \mathbf{X})[K(\mathbf{X}, \mathbf{X}) + \sigma_n^2 I]^{-1} K(\mathbf{X}, \mathbf{X}^*),$$
(2)

where σ_n^2 is the measurement noise variance.

In order for the GP to be a generative model of the data, the hyperparameters θ must be chosen appropriately. If these are not known in advance, they can be learned by maximizing the log marginal likelihood of the observations. The optimal hyperparameters can be found as

$$\theta^* \in \operatorname{argmax}_{\theta \in \mathbb{R}^p} \{ -\frac{1}{2} \mathbf{y}^T K^{-1} \mathbf{y} - \frac{1}{2} \log |K| \},$$
 (3)

where |K| represents the determinant of K. The objective function in Eq. (3) can be optimized via gradient methods [24]. Note that since this is a non-convex problem, the resulting θ^* is usually computed using multi-start gradient ascent.

III. PROBLEM STATEMENT AND MULTIFIDELITY MODEL

A. Problem Statement

We consider an autonomous marine vehicle that moves in a 3D space. The vehicle is tasked with sampling and reconstructing a static scalar measurement field using a point sensor, with resource constraints such as a budget on the total time or total energy. We assume that there exists a measurement model

$$\bar{\nu} = f(\mathbf{x}),\tag{4}$$

where $f(\mathbf{x}) : \mathbb{R}^d \to \mathbb{R}$ is an unknown function that perfectly describes the measurement field with input \mathbf{x} . We also assume that its measurement $\tilde{\nu}$ at any \mathbf{x} is corrupted by a zero mean Gaussian noise ϵ_u with variance σ_n^2 , i.e.,

$$\tilde{\nu} = f(\mathbf{x}) + \epsilon_y. \tag{5}$$

In this work, the measurement field is assumed to be invariant of the vehicle's depth¹ and the input x is the location of the vehicle on the horizontal plane (x, y). The vehicles often experience localization errors when sensing underwater due to the loss of GPS signal. We assume that the robot can perfectly access its location in the horizontal plane only at the surface of the body of water. When below the water surface, the vehicle is assumed to only have an estimate $\hat{\mathbf{x}} = \mathbf{x} + \epsilon_{\mathbf{x}}$ (generated from a state estimator such as a Kalman filter) of its true location x. Here, ϵ_x is the estimation error whose variance increases with time spent underwater after the last surfacing. As a result, the dataset $z = (y, \hat{X})$ is collected, where y is defined as in Section II and $\hat{\mathbf{X}} = [\hat{\mathbf{x}}^{[1]}, ..., \hat{\mathbf{x}}^{[n]}]^T$. Using the dataset \mathbf{z} and hyperparameters θ , an estimate $\hat{f}_{\mathbf{z}}(\mathbf{x})$ of the measurement field $f(\mathbf{x})$ can be constructed using GP regression.

The goal of this work is to design an adaptive sampling strategy that incorporates measurements along the vehicle's trajectory (including those collected underwater) to improve the reconstruction performance as measured via root-meansquared error (RMSE). The problem can be formulated as

¹The vehicles are assumed to have motion constraints that require them to change depth. This is the case for robots such as underwater gliders and gliding robotic fish.

selecting a discretized trajectory² $\mathcal{X} = [x_1, x_2, ..., x_N]$ that minimizes the RMSE between the true field $\mathbf{f}(\mathcal{D}) \in \mathbb{R}^{|\mathcal{D}|}$ and an estimate $\hat{\mathbf{f}}_{\mathbf{z}}(\mathcal{D}, \mathcal{X}) \in \mathbb{R}^{|\mathcal{D}|}$ of the measurement field for each $\mathbf{x} \in \mathcal{D}$ given a trajectory \mathcal{X} , subject to a finite budget B on the total available resources for motion, such as energy or time. Here $|\mathcal{D}|$ is the cardinality of the set \mathcal{D} of all positions in a finite space of interest. In practice, we take \mathcal{D} as a uniform grid that sufficiently covers the space of interest. $\mathbf{f}(\mathcal{D}) \in \mathbb{R}^{|\mathcal{D}|}$ and $\hat{\mathbf{f}}_{\mathbf{z}}(\mathcal{D}, \mathcal{X})$ are column vectors containing values of the true field $f(\mathbf{x})$ and its estimate $\hat{f}_{\mathbf{z}}(\mathbf{x})$ based on the trajectory \mathcal{X} , respectively, evaluated at all points $\mathbf{x} \in \mathcal{D}$. The problem can be written as

$$J(\mathcal{X}^*) \in \operatorname{argmin}_{\mathcal{X}} \mathbb{E} \left[\sqrt{\frac{1}{|\mathcal{D}|} \sum_{i=1}^{|\mathcal{D}|} (f(\mathcal{D}_i) - \hat{f}_z(\mathcal{D}_i, \mathcal{X}))^2} \right]$$

subject to

$$\sum_{i=1}^{N} S(x_i, x_{i-1}) \le B,$$

(6)

where \mathcal{D}_i is an element of \mathcal{D} , $\hat{f}_z(\mathcal{D}_i,\mathcal{X})$ is the estimate of true field predicted at a location \mathcal{D}_i conditioned on the trajectory \mathcal{X} , and $S(x_{i-1},x_i)$ is the resource consumed while moving between x_{i-1} and x_i . Note that the trajectory \mathcal{X} will be subject to constraints based on dynamics of the chosen vehicle, but we forego explicitly discussing these to place focus on the proposed usage of the multifidelity GP model and the adaptive sampling algorithm.

When using a zero-mean GP prior with a measurement field whose value is zero throughout most of the field, the RMSE can be deceptive. To avoid this issue, δ -RMS is introduced. δ -RMS is the RMSE disregarding locations where the magnitude of both the true field and the estimated field prediction are less than some $\delta > 0$. It is calculated as

$$\delta_{RMS} = \sqrt{\frac{\sum_{i=1}^{|\mathcal{D}|} \mathcal{I}_i(\mathbf{f}(\mathcal{D}), \hat{\mathbf{f}}_z(\mathcal{D}), \delta) (f(\mathcal{D}_i) - \hat{f}_z(\mathcal{D}_i))^2}{\sum_{i=1}^{|\mathcal{D}|} \mathcal{I}_i(\mathbf{f}(\mathcal{D}), \hat{\mathbf{f}}_z(\mathcal{D}), \delta)}},$$

where $\mathcal{I}(\zeta_1,\zeta_2,\delta)$ is an indicator function that produces a column vector whose i-th entry satisfies $\mathcal{I}_i = (\sqrt{\zeta_{1i}^2} > \delta) \lor (\sqrt{\zeta_{2i}^2} > \delta)$ and \lor is the logical or operation.

B. Multifidelity Model

One drawback of GP regression is that it assumes the input $\mathbf x$ to be precisely known. For this work, the input is perturbed by the estimation error $\epsilon_{\mathbf x}$. It is shown in [7] that if the measurements in a GP are accessed with inputs perturbed by a Gaussian noise, then these measurements correspond to another GP defined over perturbed inputs. These perturbed inputs lead to a warped prediction of the measurement field when using a GP, but the robot needs to accurately predict the true function $\bar{\nu} = f(\mathbf x)$ for each location $\mathbf x \in \mathcal D$ to effectively plan new sample locations. The estimation error $\epsilon_{\mathbf x}$ corresponds to variable levels of uncertainty on the

position estimate $\hat{\mathbf{x}}$. The dataset $\mathbf{z} = (\mathbf{y}, \hat{\mathbf{X}})$ can be split into separate datasets based on the level of uncertainty in $\hat{\mathbf{X}}$. This motivates the idea of using a multifidelity GP to create the estimate $\hat{f}_{\mathbf{z}}(\mathbf{x})$ for all $\mathbf{x} \in \mathcal{D}$ of the measurement field.

We propose a multifidelity GP representation of the field whose fidelity levels are dependent on the localization uncertainty. In the proposed approach, uncertainty in the location estimates are binned into M+1 fidelity levels, where uncertainty increases with the fidelity level, i.e, level 0 corresponds to the lowest uncertainty. Multiple datasets $(\mathbf{y}_i, \hat{\mathbf{X}}_i)$ are constructed where measurements and input locations are assigned to a particular dataset based on the uncertainty in the input location. Each dataset will be used to construct a corresponding Gaussian process and these GPs are coupled through a nested structure on their means and covariance. The proposed model is consistent with the recursive auto-regressive multifidelity model³

$$f_i(\mathbf{X}) = \rho_{i+1}(\mathbf{X}) f_{i+1}(\mathbf{X}) + \xi_{i+1}(\mathbf{X}),$$
 (7)

presented in [18], where ξ_i are bias terms that are independent from levels of lower fidelity. The mean of the GP at each fidelity level is expressed as

$$\mu_i(\mathbf{X}^*) = \rho_{i+1}(\mathbf{X}^*)\mu_{i+1}(\mathbf{X}^*) + K_i(\mathbf{X}^*, \mathbf{X}_i)K_i(\mathbf{X}_i, \mathbf{X}_i)^{-1}(\mathbf{y}_i - \rho_{i+1}(\mathbf{X}_i)\mu_{i+1}(\mathbf{X}_i)),$$
(8)

for some fidelity i, $0 \le i \le M$, where M+1 is the total number of GP models considered. The functions $\rho_i(\mathbf{X})$ are scaling coefficients relating the outputs \mathbf{y}_i of the different fidelity levels and K_i is the kernal for ξ_{i+1} . The variance at each fidelity level is calculated as

$$\Sigma_i(\mathbf{X}^*) = \bar{\Sigma}_i(\mathbf{X}^*) + \rho_{i+1}^2(\mathbf{X}^*)\bar{\Sigma}_{i+1}(\mathbf{X}^*), \tag{9}$$

where $\bar{\Sigma}_i$, for i=0,...,M is calculated using Eq. (2) and the appropriate dataset $(\mathbf{y}_i,\mathbf{X}_i)$. The GPs and datasets $(\mathbf{y}_i,\mathbf{X}_i)$ are assumed to be ordered according to increasing levels of uncertainty in the position estimate with \mathbf{GP}_0 corresponding to the data associated with the measured positions which are assume to have the highest certainty. \mathbf{GP}_M will be considered as a constant, zero-mean function. The predictive mean and the variance of the multifidelity GP are taken as

$$\mu_{MF}(\mathbf{X}^*) = \mu_0(\mathbf{X}^*),\tag{10}$$

$$\Sigma_{MF}(\mathbf{X}^*) = \Sigma_0(\mathbf{X}^*) \tag{11}$$

with $\mu_0(\mathbf{X}^*)$ and $\Sigma_0(\mathbf{X}^*)$ calculated as in Eqs. (8) and (9). In the next section, we describe an algorithm that uses the multifidelity model to collect data and build a spatial map while exploring an initially unknown measurement.

IV. ADAPTIVE SAMPLING ALGORITHM

The psuedo code for the adaptive sampling algorithm is given in Algorithm 1. The algorithm takes as inputs the initial robot position p_0 , an expected information density

²Note that elements of \mathcal{X} in \mathbb{R}^3 , but only the horizontal components are used in $\hat{f}_{\mathbf{z}}$

³The original auto-regressive model presented in [17] takes $\rho_i(\mathbf{X})$ as constants that can be learned along with the covariance kernel hyperparameters. This is generalized to an input-dependent function in [18].

(EID) $\Phi(x)$, a number n_s of sample points to be planned, a list of user-defined fidelity level thresholds that are used to assign data, a budget function $\mathbf{S}(\mathcal{X}) = \sum_{i=1}^N S(x_i, x_{i-1})$ on the trajectory \mathcal{X} and a budget constraint B on the available resource. The EID is an important part of the algorithm that drives the exploration. Several quantities such as Fisher information, the upper confidence bound, mutual information, or entropy may be used to construct the EID. Here, it is based on the multifidelity mean (Eq. (10)) and variance (Eq. (11)) and will be defined later (see Eq. (13)).

The algorithm plans the sample points on a rectangular domain $\mathcal{D} = [L_1 \times L_2]$ and calculates a path that visits each sample point. The SelectSamplePoints function outputs an ordered set of n_s sample locations that form the path. The robot follows the path collecting data at the selected sample locations and intermediate locations along the path. The robot maintains an estimate of its position \hat{p} and the collected data $(\tilde{\nu}, \hat{p})$ is assigned to an appropriate fidelity level by comparing the quantity $\eta_{\hat{p}}$ (representing the amount of uncertainty in the localization) to the user-defined thresholds $[\phi_0, ..., \phi_{m-1}]$. The robot is required to sample the n_s sample locations from the SelectSamplePoints function at high fidelity by returning to the surface. The GOTO function assumes that there is a controller capable of handling the navigation of the robot to the sampling locations. Localization error may cause the robot to surface at an incorrect location. In this case, the robot will then proceed to navigate to the correct location o the surface. After all sample points have been visited, the Gaussian process is updated with the new data and the hyperparameters of the Gaussian processes are trained in reverse sequence (i.e θ_{M-1} , $\theta_{M-2},...,\theta_0$) according to Eq. (3). This is a heuristic that treats $f_i(x) - \rho_{i+1}\mu_{i+1}(X)$ as a measurement of ξ_{i+1} . Then a new set of sample points are selected based on the updated EID. The process is repeated until the resource is exhausted. The next section explains the sample selection process.

A. Sampling and Path Planning Algorithm

This work uses the ergodic metric proposed by [23] to plan the sample points to visit. The metric compares the spatial statistics of a trajectory to a spatial distribution of an EID, naturally balancing exploration and exploitation. Minimizing the metric leads to a trajectory that distributes time spent in specific regions of the domain proportionally to the information in those regions [25], [26].

The ergodic metric is given by [23]

$$\omega(x(t)) = \sum_{k=0}^{\mathcal{K}} \Delta_k |c_k(x(t)) - \Phi_k|^2$$
 (12)

where Φ_k and c_k are the Fourier coefficients of basis functions approximating a spatial distribution $\Phi(x)$ and a time-averaged trajectory x(t), respectively. $\mathcal K$ determines the number of coefficients used to measure the distance from ergodicity along each dimension of a n-dimesional rectangular domain and $k \in \mathcal K$ is a multi-index $(k_1, k_2, ..., k_n)$. The coefficients can be calculated as $\Phi_k = \int_x \Phi(x) F_k(x) dx$ and $c_k = \int_x \Phi(x) F_k(x) dx$

Algorithm 1

```
Input:
```

```
Initial robot pose p_0
Domain of exploration \mathcal{D}
Expected information density \Phi(\mathcal{D})
Number of planned sample points locations n_s
Gaussian Process fidelity thresholds [\phi_0,\phi_1,...,\phi_{M-1}]
Budget constraint B
Budget \mathbf{S}(\mathcal{X})
```

```
1: \hat{p} \leftarrow p_0
 2: \mathcal{X} \leftarrow \{\hat{p}\}
 3: (\mathbf{y}_i, \hat{\mathbf{X}}_i) \leftarrow \{\} for i = 0, ..., M
 4: X_s \leftarrow \text{SelectSamplePoints}(\mathcal{X}, \Phi(\mathcal{D}))
 5: i_s \leftarrow 0
 6: x_s \leftarrow X_s[i_s]
 7: while B > \mathbf{S}(\mathcal{X}) do
               if ||\hat{p} - x_s|| < \epsilon then
                       i_s \leftarrow i_s + 1
 9:
                       if i_s > n_s then
10:
                              X_s \leftarrow \text{SelectSamplePoints}(\mathcal{X}, \Phi(\mathcal{D}))
11:
                              i_s \leftarrow 0
12:
                       x_s \leftarrow X_s[i_s]
13:
               if \eta_{\hat{p}} \leq \phi_0 then
14:
                       (\mathbf{y}_0, \mathbf{\hat{X}}_0) \leftarrow (\mathbf{y}_0, \mathbf{\hat{X}}_0) \cup \{(\tilde{\nu}, \hat{p})\}
15:
               else if \phi_k \leq \eta_{\hat{p}} \leq \phi_{k+1} then
16:
                       (\mathbf{y}_{k+1}, \hat{\mathbf{X}}_{k+1}) \leftarrow (\mathbf{y}_{k+1}, \hat{\mathbf{X}}_{k+1}) \cup \{(\tilde{\nu}, \hat{p})\}\
17:
               GOTO(\hat{p}, x_s)
18:
               Update \hat{p}
19:
               \mathcal{X} \leftarrow \mathcal{X} \cup \{\hat{p}\}
20:
```

 $\frac{1}{T}\int_{t_0}^{t_0+T}F_k(x(t))dt$, where $F_k(x)=\frac{1}{h_k}\prod_{i=1}^n\cos(\frac{k_i\pi}{L_i}x_i)$ are the Fourier basis functions used to approximate the spatial distribution $\Phi(x)$ and the trajectory x(t) over n dimensions. h_k is a normalizing factor and x_i is the i-th component of x. $\Delta_k=\frac{1}{(1+||k||^2)^{\frac{n+1}{2}}}$ is used to place larger weight on lower frequency information. The reader is referred to [23], [26] for more details on the ergodic metric.

In the SelectSamplePoints function, the ergodic metric is used to select a finite number of sample locations given the robot's current trajectory x(t). While in theory x(t)is a continuous function, in practice, it is approximated by \mathcal{X} . Population-based optimization techniques are used to generate sets of sampling points. Then the algorithm estimates the trajectory taken to reach the sampling points by assuming a constant speed through an open Traveling Salesman Tour over the graph of sample points with edges being the distances between points. The set of sampling points that results in the minimum value for the ergodic metric is chosen. The spatial distribution $\Phi(x)$ used to drive the exploration is based on the multifidelity mean (Eq. (10)) and variance (Eq. (11)). It is chosen as a combination of the mean and variance in order to treat unsampled locations and locations with a large mean as informative locations. It is calculated as

$$\Phi(\mathbf{x}) = \alpha \mu_{MF}(\mathbf{x}) + (1 - \alpha)\bar{\Sigma}_{MF}(\mathbf{x})$$
 (13)

for each point $\mathbf{x} \in \mathcal{D}$, where $\alpha \in [0,1]$ is a parameter to be chosen by a user and

$$\bar{\Sigma}_{MF}(\mathbf{x}^*) = \bar{\Sigma}_0(\mathbf{x}^*) + \sum_{i=1}^M \frac{\prod_{j=0}^i \bar{\Sigma}_j(\mathbf{x}^*)}{\prod_{j=0}^{i-1} \max(\bar{\Sigma}_j(\mathcal{D}))}, \quad (14)$$

where $\bar{\Sigma}_i$, for i = 0, ..., M is calculated as

$$\bar{\Sigma}_i = K_i(\mathbf{X}^*, \mathbf{X}^*) - K_i(\mathbf{X}^*, \mathbf{X}_i) K_i(\mathbf{X}_i, \mathbf{X}_i)^{-1} K(\mathbf{X}_i, \mathbf{X}^*),$$

 $\bar{\Sigma}_{MF}$ pre-multiplies lower fidelity predictive variance with the normalized predictive variances of all higher fidelity models. Eq. (14) encodes a heuristic rule: measurements associated with higher uncertainty in the location are less informative if that location has been measured with lower uncertainty in the location. As an example, Eq. (14) becomes

$$\begin{split} \bar{\Sigma}_{MF}(\mathbf{x}) &= \bar{\Sigma}_0(\mathbf{x}) + \frac{\bar{\Sigma}_0(\mathbf{x})}{\max(\bar{\Sigma}_0(\mathcal{D}))} \bar{\Sigma}_1(\mathbf{x}) \\ &+ \frac{\bar{\Sigma}_0(\mathbf{x})\bar{\Sigma}_1(\mathbf{x})}{\max(\Sigma_0(\mathcal{D}))\max(\bar{\Sigma}_1(\mathcal{D}))} \bar{\Sigma}_2(\mathbf{x}) \end{split}$$

with two fidelity levels. Note that the EID need not change with time in general, but does so here because the Gaussian process is updated with the data collected at each point along the trajectory $\mathcal X$ after reaching all of the selected sample locations.

The next section discusses simulation of the adaptive sampling algorithm and compares the reconstruction performance of the proposed multifidelity GP to two alternative methods.

V. SIMULATION STUDY

A. Setup

In simulation, a measurement field is generated by placing H sources in a $20{\times}40$ meter rectangular domain. The source intensities are generated using the formula $f(x_p) = \sum_{h=1}^{H} s_1 e^{(-(s_2(x_h-x_p))^2)}$ where $x_p \in R^2$ is the position of the robot and x_h is one of H source locations within the field. s_1 and s_2 are positive constants. For the simulations in this work, H, s_1 , and s_2 are chosen as 5, 10, and 0.5, respectively.

The gliding robotic fish is chosen as the robot to be simulated in the space. Details on the dynamic model can be found in [15], [27]. Algorithm 1 is applied as the exploration strategy for the robot with B=150 minutes being a fixed time limit. We take $n_s=10$ as the number of sample points to plan during each planning step. The cost of traveling to all n_s sample points depends on the robot's speed and the distances between the planned sample points. While traveling between sampling locations, the robot glides between the surface and a prescribed reference depth with fixed reference pitch angles as depicted in Fig. 1, which is a standard behavior for the robot. The localization uncertainty will periodically be reset to zero whenever the robot surfaces and grow once underwater again. Here, the prescribed depth,

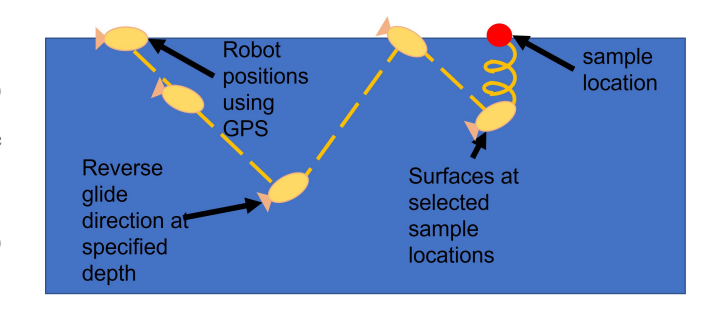


Fig. 1. Depiction of gliding robotic fish navigating to a sampling location. Intermediate measurements taken between sample locations may be assigned to imprecise locations due to loss of GPS.

is chosen so that the robot is unlikely to surface between sampling points. When the robot is believed to be at a selected sampling location, it is required to collect a sample at the surface which causes it to surface if underwater. The robot's position is estimated via an extended Kalman filter using model parameters that were randomly perturbed with a maximum of 2% from their true values.

The multifidelity Gaussian process model described in Section III-B with $\rho(\mathbf{X}) = 1$ is used to reconstruct the field based on the location and intensity measurements. The covariance used for the GP is the squared exponential kernel, with entries $K_{ij}(\mathbf{x}_i, \mathbf{x}_j) = \sigma_s e^{-(\mathbf{x}_i - \mathbf{x}_i)^T \Delta_l^{-1}(\mathbf{x}_i - \mathbf{x}_j)}$, where Δ_l is an identity matrix multiplied by the inverse of the squared length scale and σ_s is the signal noise. The number M of fidelity levels is taken as 5. A data pair (y_i, X_i) is assigned to a dataset by comparing the value $\eta_{\hat{p}}$ in Algorithm 1 to the thresholds ϕ_i , i=0,...,M-1for the fidelity levels. Here the average standard deviation of the expected localization error, $\eta_{\hat{p}} = \text{mean}(\sqrt{\text{diag}(P_{xy})})$ is used to determine the appropriate dataset. P_{xy} is the submatrix of the estimation error covariance matrix from the extended Kalman filter associated with the (x, y) position. The vector to assign the fidelity level is taken as a percentage of the smallest dimension of the domain (e.g., 20 m). The percentages are chosen as [2.5%, 7.5%, 10%, 15%, 25%].

The simulation is run 50 times with a start location of (0,0), fixed source locations, and a fixed perturbation to the model parameters for the robot. After the simulations are run, the field reconstruction performance of the proposed multifidelity model is compared with two other methods:

- 1) Noisy input single fidelity (NISF), which ignores localization errors and adds all data to a single GP model,
- Disregarded low fidelity (DLF), which throws out lower fidelity measurements and only uses the data with known location in a single GP model.

B. Results

The performance is measured in terms of the δ -RMS error (see Section III) for the field reconstruction with $\delta=0.005$. The different field representations are compared to the true field and to a GP reconstruction using perfect inputs for all collected data termed the perfect input (PI) GP model. While the hyperparameters were tuned online for the proposed

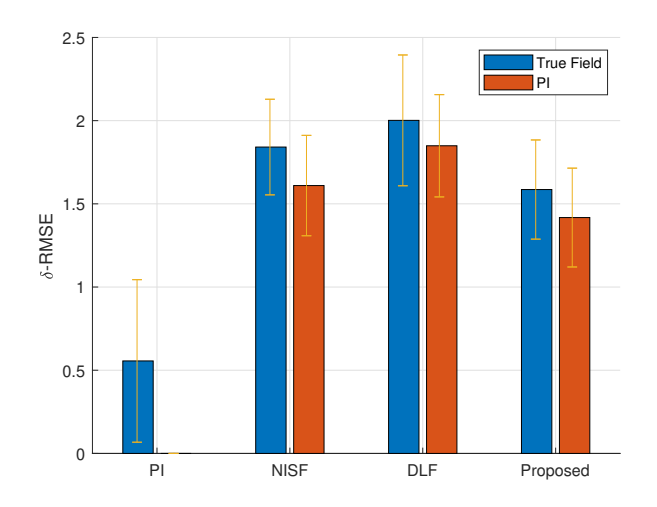


Fig. 2. Mean and standard deviation over 50 trials for δ -RMS reconstruction error comparison for each method with baselines being a Gaussian process with perfect input for all collected data (PI) and the true field.

 $\label{eq:table in table in table is solution} TABLE\ I$ $\delta\text{-RMS}$ reconstruction error comparison Simulation in Figs. 3 and 4

Model/	PI	NISF	DLF	Prop
Baseline				
True Field	0.0868	1.6618	2.2959	1.1672
PI	0	1.6383	2.2116	1.1617

approach, they are re-tuned offline using all of the collected data with the same initialization strategy as used in the other methods for fair comparison. Fig. 2 shows the average δ -RMS reconstruction error with error bars depicting the standard deviation for each method after the 50 trials. It also shows the average RMS reconstruction error for the GP with perfect input for comparison. Out of the 50 trials, the RMS error was lower for the proposed method than for NISF 42 of 50 times when compared to the true field and 40 times when compared to the Gaussian process with perfect input (PI). The RMS error was lower than the DLF model 44 of 50 times and 42 of 50 times, respectively. The DLF model had a lower RMS error than NISF model 15 of 50 times when compared to the Gaussian process with perfect input (PI).

Table I and Figs. 3 and 4 show the results from a single trial. In this trial, the robot successfully plans two sets of points. Fig. 4(b) shows the robot's path only through the first set of planned sample locations to highlight how the position estimate $\hat{\mathbf{x}}$ drifts from the true position \mathbf{x} in 3 dimensions. Table I shows that the path is sufficient for reconstructing the field with low error if the location is perfectly known. However, localization error degrades the reconstruction performance.

All of the GP models initially predict a zero-mean, constant variance across the field making the first set of sample points distributed approximately uniformly throughout the field. In Fig. 4, it can be seen that most of the sampling

points lie outside of the contours for the source intensities. As shown in Fig. 3, this causes the DLF model (which disregards low fidelity measurements) to predict low values or even zero values in places where sources are located despite the robot passing nearby. The NISF model better predicts the locations around the sources because it includes all of the data. However, the localization error causes artifacts that do not exist to be predicted. The proposed method predicts similarly to the NISF model, but some artifacts due to localization errors are removed when high-fidelity measurements are taken at nearby locations. This results in the proposed model having a lower RMS reconstruction error than both the NISF model and the DLF model.

Fig. 5 shows how the δ -RMS reconstruction error changes when the localization error $\epsilon_{\mathbf{x}}$ is scaled by a constant factor for both the proposed multifidelity model and the NISF model. For each scaling factor, the hyperparameters are retrained on both models. Both show an approximately linear growth with the scaling factor, but the proposed method produces the lower δ -RMSE for most. The exception is that with perfect localization, the NISF model produces a slightly lower δ -RMSE.

In addition to slightly better performance in the reconstruction error, the proposed approach has a theoretical advantage over the NISF GP model due to the Cholesky decomposition used to compute the inverse of the covariance matrix K in the GP prediction equations (Eqs. (1) and (2)). The data is assigned to each fidelity level i in the propsed approach such that $N = \sum_{i=0}^{M} n_i$ where n_i is the number of samples in a fidelity level i and N is the number of samples collected over the course of the robot's trajectory. Because the proposed approach uses a recursive prediction, its computational complexity is dependent on $\sum_{i=0}^{M} n_i$ compared to $(\sum_{i=0}^{M} n_i)^3$ for the NISF GP model. Taking n_i to be equal for all i leads to a big-O notation of $O(M^3 n_i^3)$ for the latter and $O(M n_i^3)$ for the former.

VI. CONCLUSION AND FUTURE WORK

In this work, we proposed multifidelity Gaussian process regression as the basis of an adaptive sampling algorithm that incorporates localization uncertainties. The approach was shown to improve field reconstruction over an approach that ignores localization error and an approach that ignores low-fidelity data. The results suggest the proposed approach is promising for incorporating intermediate, low-quality data into adaptive sampling schemes.

In future work, we plan to theoretically analyze the approach and also include learning the scaling functions $\rho_i(x)$. In addittion, we plan to extend the approach to work with measurement fields that vary with 3-dimensional space, analyze the adaptive sampling algorithm, evaluate the performance of the adaptive sampling algorithm using the different Gaussian process models to represent the field, and conduct experiments on a physical robot [16], [27]. Another future direction of this work entails designing an algorithm to improve the lower certainty position estimates based on the surfacing locations of the robot in order to improve

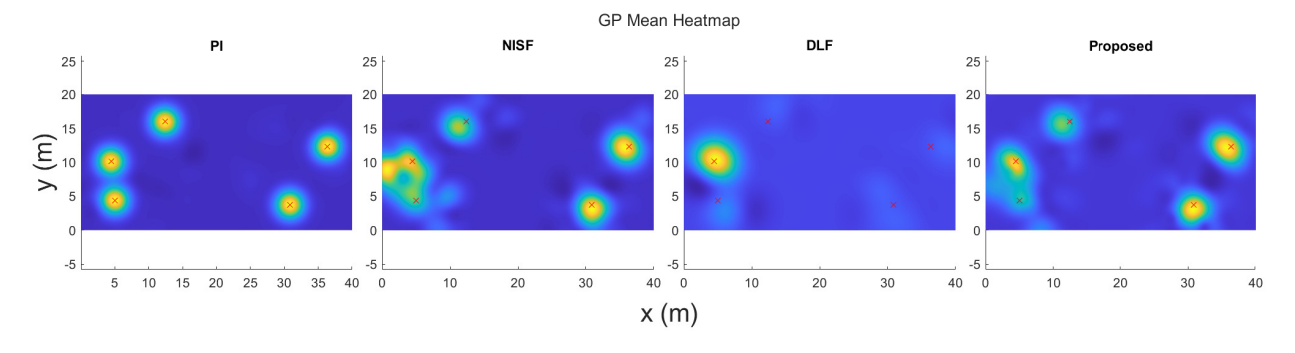
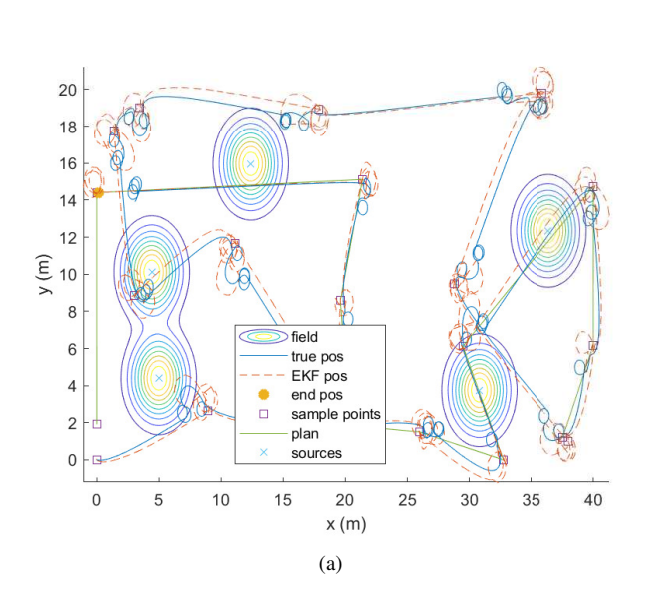


Fig. 3. Heat maps of the reconstruction for each Gaussian process model. Blue indicates lower values and the crosses indicate the source locations.



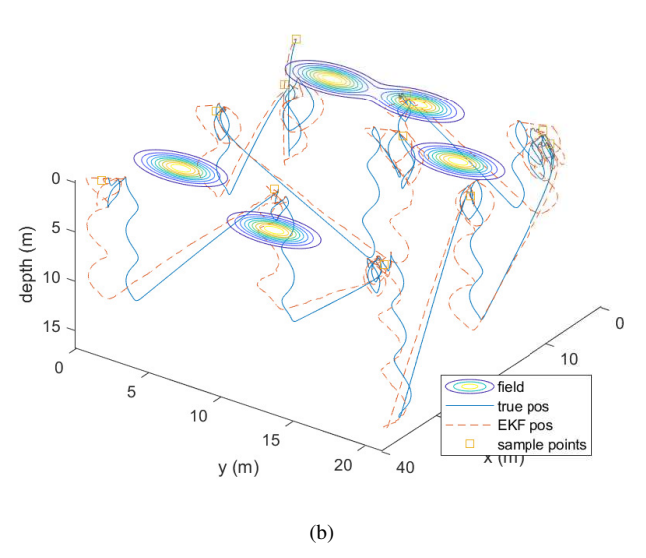


Fig. 4. Depiction of the robot path from top down (top) and 3D (bottom) views. The solid line represents the true path of the robot while the dashed line represents the estimated path. "Plan" refers to the planned path of the current set of sampling points.

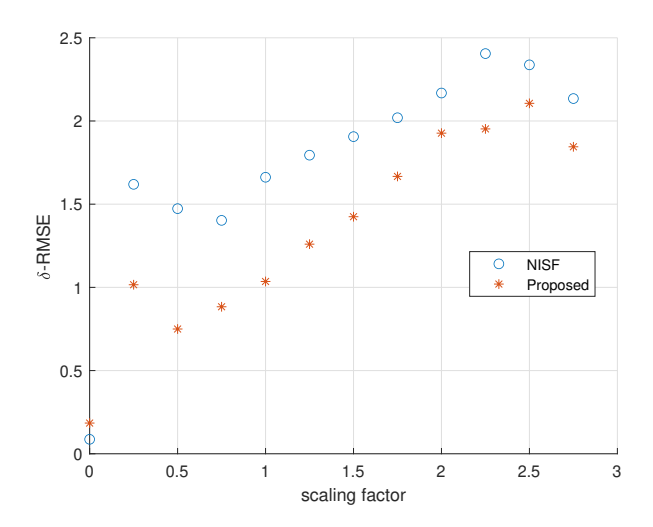


Fig. 5. δ -RMS for NISF and proposed model when compared to the true field with the localization error scaled by a constant factor.

prediction performance. It is also of interest to combine the proposed scheme with the noisy input Gaussian process framework described in [9] to improve performance and compare single and multifidelity approaches.

REFERENCES

- F. Hidalgo and T. Bräunl, "Review of underwater SLAM techniques," in 2015 6th International Conference on Automation, Robotics and Applications (ICARA). IEEE, 2015, pp. 306–311.
- [2] A. Murphy, M. Landamore, and R. Birmingham, "The role of autonomous underwater vehicles for marine search and rescue operations," *Underwater Technology*, vol. 27, no. 4, pp. 195–205, 2008.
- [3] L. Wei, X. Tan, and V. Srivastava, "Expedited multi-target search with guaranteed performance via multi-fidelity gaussian processes," in 2020 IEEE/RSJ International Conference on Intelligent Robots and Systems (IROS). IEEE, 2020, pp. 7095–7100.
- [4] O. Ennasr, G. Mamakoukas, T. Murphey, and X. Tan, "Ergodic exploration for adaptive sampling of water columns using gliding robotic fish," in *Dynamic Systems and Control Conference*, vol. 51913. American Society of Mechanical Engineers, 2018, p. V003T32A016.
- [5] M. Jadaliha, Y. Xu, J. Choi, N. S. Johnson, and W. Li, "Gaussian process regression for sensor networks under localization uncertainty," *IEEE Transactions on Signal Processing*, vol. 61, no. 2, pp. 223–237, 2012.
- [6] S. Choi, M. Jadaliha, J. Choi, and S. Oh, "Distributed Gaussian process regression under localization uncertainty," *Journal of Dynamic Systems, Measurement, and Control*, vol. 137, no. 3, p. 031007, 2015.

- [7] D. Cervone and N. S. Pillai, "Gaussian process regression with location errors," arXiv preprint arXiv:1506.08256, 2015.
- [8] H. Bijl, T. B. Schön, J.-W. van Wingerden, and M. Verhaegen, "Online sparse Gaussian process training with input noise," ArXiv, vol. abs/1601.08068, 2016.
- [9] A. McHutchon and C. Rasmussen, "Gaussian process training with input noise," Advances in Neural Information Processing Systems, vol. 24, 2011.
- [10] R. Oliveira, L. Ott, and F. Ramos, "Bayesian optimisation under uncertain inputs," in *The 22nd International Conference on Artificial Intelligence and Statistics*. PMLR, 2019, pp. 1177–1184.
- [11] P. Dallaire, C. Besse, and B. Chaib-Draa, "An approximate inference with Gaussian process to latent functions from uncertain data," *Neu-rocomputing*, vol. 74, no. 11, pp. 1945–1955, 2011.
- [12] H. Stommel, "The Slocum Mission," Oceanography, vol. 2, no. 1, pp. 22–25, 1989.
- [13] J. Sherman, R. E. Davis, W. Owens, and J. Valdes, "The autonomous underwater glider "Spray"," *IEEE Journal of Oceanic Engineering*, vol. 26, no. 4, pp. 437–446, 2001.
- [14] J. Sliwka, B. Clement, and I. Probst, "Sea glider guidance around a circle using distance measurements to a drifting acoustic source," in *Intelligent Robots and Systems (IROS)*, 2012 IEEE/RSJ International Conference on. IEEE, 2012, pp. 94–99.
- [15] F. Zhang, "Modeling, design and control of gliding robotic fish," Dissertation, Michigan State University. Electrical Engineering, 2014.
- [16] O. N. Ennasr, "Gliding robotic fish: Design, collaborative estimation, and application to underwater sensing," Ph.D. dissertation, Michigan State University, 2020.
- [17] M. C. Kennedy and A. O'Hagan, "Predicting the output from a complex computer code when fast approximations are available," *Biometrika*, vol. 87, no. 1, pp. 1–13, 2000.
- [18] L. Le Gratiet and J. Garnier, "Recursive co-kriging model for design of computer experiments with multiple levels of fidelity," *International Journal for Uncertainty Quantification*, vol. 4, no. 5, 2014.
- [19] L. Brevault, M. Balesdent, and A. Hebbal, "Overview of Gaussian process based multi-fidelity techniques with variable relationship between fidelities, application to aerospace systems," *Aerospace Science* and Technology, vol. 107, p. 106339, 2020.
- [20] S. Ficini, U. Iemma, R. Pellegrini, A. Serani, and M. Diez, "Assessing the performance of an adaptive multi-fidelity gaussian process with noisy training data: A statistical analysis," in AIAA AVIATION 2021 FORUM, 2021, p. 3098.
- [21] S. Ficini, R. Pellegrini, A. Odetti, A. Serani, U. Iemma, M. Caccia, and M. Diez, "Uncertainty quantification of an autonomous surface vehicle by multi-fidelity surrogate models," in 9th edition of the International Conference on Computational Methods for Coupled Problems in Science and Engineering (COUPLED PROBLEMS 2021), 2021.
- [22] Y. Sung, D. Dixit, and P. Tokekar, "Environmental hotspot identification in limited time with a UAV equipped with a downward-facing camera," in 2021 IEEE International Conference on Robotics and Automation (ICRA). IEEE, 2021, pp. 13264–13270.
- [23] G. Mathew and I. Mezić, "Metrics for ergodicity and design of ergodic dynamics for multi-agent systems," *Physica D: Nonlinear Phenomena*, vol. 240, no. 4-5, pp. 432–442, 2011.
- [24] C. K. Williams and C. E. Rasmussen, *Gaussian processes for machine learning*. MIT press Cambridge, MA, 2006, vol. 2, no. 3.
- [25] L. M. Miller and T. D. Murphey, "Trajectory optimization for continuous ergodic exploration," in 2013 American Control Conference. IEEE, 2013, pp. 4196–4201.
- [26] A. Mavrommati, E. Tzorakoleftherakis, I. Abraham, and T. D. Murphey, "Real-time area coverage and target localization using receding-horizon ergodic exploration," *IEEE Transactions on Robotics*, vol. 34, no. 1, pp. 62–80, 2017.
- [27] D. Coleman, M. Castaño, and X. Tan, "Backstepping control of gliding robotic fish for pitch and 3D trajectory tracking," *Control Engineering Practice*, vol. 129, p. 105350, 2022.